Defining the ferroptotic phenotype of beta cells in type 1 diabetes and its inhibition as a potential antidiabetic strategy

Milica Markelic[1]*, Ana Stancic[2], Tamara Saksida[3], Ilijana Grigorov[2], Dragica Micanovic[3], Ksenija Velickovic[1], Vesna Martinovic[2], Nevena Savic[2], Andjelija Gudelj[2] and Vesna Otasevic[2]*

[1]Department of Cell and Tissue Biology, Faculty of Biology, University of Belgrade, Serbia, [2]Department of Molecular Biology, Institute for Biological Research "Siniša Stanković", National Institute of Republic of Serbia, University of Belgrade, Belgrade, Serbia, [3]Department of Immunology, Institute for Biological Research "Siniša Stanković", National Institute of Republic of Serbia, University of Belgrade, Belgrade, Serbia

Introduction: Recently, the involvement of ferroptotic cell death in the reduction of β-cell mass in diabetes has been demonstrated. To elucidate the mechanisms of β-cell ferroptosis and potential antidiabetic effects of the ferroptosis inhibitor ferrostatin-1 (Fer-1) in vivo, a mouse model of type 1 diabetes (T1D) was used.

Methods: Animals were divided into three groups: control (vehicle-treated), diabetic (streptozotocin-treated, 40 mg/kg, from days 1-5), and diabetic treated with Fer-1 (1 mg/kg, from days 1-21). On day 22, glycemia and insulinemia were measured and pancreases were isolated for microscopic analyses.

Results: Diabetes disturbed general parameters of β-cell mass (islet size, β-cell abundance and distribution) and health (insulin and PDX-1 expression), increased lipid peroxidation in islet cells, and phagocytic removal of iron-containing material. It also downregulated the main players of the antiferroptotic pathway - Nrf2, GPX4, and xCT. In contrast, Fer-1 ameliorated the signs of deterioration of β-cell/islets, decreased lipid peroxidation, and reduced phagocytic activity, while upregulated expression of Nrf2 (and its nuclear translocation), GPX4, and xCT in β-cell/islets.

Discussion: Overall, our study confirms ferroptosis as an important mode of β-cell death in T1D and suggests antiferroptotic agents as a promising strategy for the prevention and treatment of diabetes

1 Introduction

Unlike accidental cell death, which occurs immediately in response to severe chemical, physical, or mechanical insults, regulated cell death (RCD) relies on specific molecular machinery and therefore can be modulated pharmacologically or genetically (1, 2). Rather than focusing on the morphological parameters, the current classification of RCD focuses on the molecular and essential aspects, including signal transduction and the pathophysiological significance of RCD (1, 3). In this context, a necrotic form of RCD named ferroptosis was described more than a decade ago (4). It is manifested by an iron-dependent accumulation of membrane lipid peroxides. Of the processes involved in ferroptosis, the best known is the depletion of the antioxidant peptide glutathione (GSH), which leads to the failure of the lipid peroxide removal capacity of the specific membrane-associated isoform of the GSH-dependent peroxidase, GPX4 (5, 6). The main regulator of intracellular biosynthesis of GSH is a membrane Xc- glutamate/L-cystine antiporter, i.e., its light chain subunit xCT (SLC7a11) (7), which is responsible for the cellular uptake of L-cystine, which is converted to cysteine, a precursor of GSH (8). Cellular susceptibility to ferroptosis is primarily triggered by the imbalance between iron import, storage, and export, which can lead to an increase in the cytosolic labile iron pool (9). Excess cellular iron stimulates ferroptosis either directly by reacting with membrane lipids or via the iron-dependent enzymes involved in reactive oxygen species (ROS) formation and lipid peroxidation, such as lipoxygenases (10, 11). Nuclear Factor Erythroid 2–Related Factor 2 (Nrf2) is considered a master regulator of the expression of the genes related to ferroptosis, including GPX4 and SLC7a11. In addition, Nrf2 has been shown to maintain iron homeostasis by regulating the synthesis and degradation of ferritin (12).

Our understanding of ferroptosis mechanisms and its role in various diseases has been rapidly expanding. This is supported by a plethora of studies suggesting that pharmacological modulation of ferroptosis through its induction (in cancer) or inhibition (in ischemic/degenerative diseases) has potentially significant clinical utility (13). Recently, the involvement of ferroptosis in the etiology and pathogenesis of diabetes and diabetic pathologies has been proposed by several teams, including ours (14–20). Reduction of pancreatic β-cell mass is the most important pathological feature of both type 1 (T1D) and type 2 (T2D) diabetes, and the main cause is considered to be cell death (21). Although the main modules of RCD of β-cells described previously were apoptosis, necrosis, and autophagic RCD (22), in our recent study we confirmed the induction of ferroptosis under diabetogenic conditions in vitro (14). In addition, an in vivo pilot study presented in the same paper, demonstrated that ferroptosis is an important mode of β-cell death in T1D experimentally induced by streptozotocin (STZ), and suggested the use of a ferroptosis inhibitor ferrostatin-1 (Fer-1) for the protection and survival of β-cells under diabetic conditions. Fer-1 is a free-radical scavenging synthetic antioxidant that inhibits iron-dependent lipid peroxidation (23). Our preliminary in vivo results showed that Fer-1 reduced lipid peroxidation, resulting in improved islet size, increased insulin expression, and a decrease in

signs of (peri-)insulitis (14). β-Cells are considered to have low antioxidant capacity and are therefore susceptible to oxidative stress (24, 25), justifying the study of the involvement of ferroptosis as a ROS-driven RCD in the pathogenesis of diabetes.

The aim of this work is to elucidate the mechanisms of reduction in β-cell mass under diabetic conditions in vivo, including characterization of the ferroptotic phenotype in situ. In addition, we aimed to define the benefits of ferroptosis inhibition in the endocrine pancreas under diabetic conditions. For this purpose, the same ferroptosis inhibitor as in our previous in vitro and in vivo pilot study, Fer-1, was selected and. a thorough microscopic examination of pancreatic tissue from diabetic mice was performed.

2 Materials and methods

2.1 Experimental design

For this study, 8–10-week-old male C57BL/6 mice were housed in the animal facility of the Institute of Biological Research "Sinisa Stankovic" (IBISS) with unlimited access to standard food and tap water. All experimental procedures were approved by the IBISS Ethics Committee (App. No. 323-37-11487/2021-05) in accordance with Directive 2010/63/EU. Animals were divided into three groups (n = 8): diabetic (DM), diabetic Fer-1-treated (DM + Fer-1), and untreated control animals (Ctrl). For induction of diabetes, multiple low doses of STZ (40 mg/kg body mass; S0130, Sigma-Aldrich, St. Louis, MI, USA) were injected intraperitoneally (i.p.) for 5 consecutive days (days 1-5) as previously described (14). Fer-1 (1 mg/kg body mass, SML 0583, Sigma-Aldrich), dissolved in dimethyl sulfoxide (DMSO, D8418, Sigma-Aldrich) and diluted with phosphate-buffered saline (PBS), was administered i.p., starting from day 1 to 21. To avoid possible interference, the injections of STZ and Fer-1 were administered 3 h apart. The control group received the diluents in the same amount. Twenty-four hours after the last STZ and Fer-1 administration, the animals fasted for 4 h were euthanized by cervical dislocation between 9:00 and 9:30 AM. Blood and pancreas samples were collected and routinely processed for biochemical or microscopic analyses.

2.2 Measurement of serum glucose and insulin levels

Immediately after blood collection, serum was processed (26) and stored at -80°C until analysis of serum glucose level (Biochemical Laboratory "Beograd", Belgrade, Serbia) and serum insulin level (by radioimmunoassay, INEP, Belgrade, Serbia).

2.3 Microscopic examination

Immediately after dissection, pancreas pieces were sectioned and fixed overnight at 4°C in 10% formaldehyde, routinely

processed for embedding in paraffin blocks, and cut into 5 µm thin sections for microscopic analyses.

2.3.1 Histological, morphometric, and stereological analyses

For routine histological analysis and for morphometric analysis of islet surface profiles, tissue sections were routinely stained with hematoxylin and eosin (HE). In addition, AZAN trichrome staining was performed to determine the presence/stage of islet fibrosis. The islet fibrosis, reflecting extensive collagen deposition surrounding/ infiltrating islets, is visible as intensive blue staining [27] and was scored as: 0 – absent, 1 – mild, 2 – moderate, 3 – massive. For morphometric measurement of the islet surface area, approximately 50 islets per group were analysed using Image J software (NIH, USA) at a lens magnification of x 40. To detect the accumulation of iron (Fe^{3+}), Pearl's Prussian Blue staining was performed in a 2% potassium ferrocyanide solution followed by Nuclear Fast Red counterstaining. A positive reaction was detected as blue intracellular accumulation. For detection of lipofuscin, sections were stained with a 0.35% Sudan Black B (SBB) solution in 70% ethanol followed by Nuclear Fast Red counterstaining. A positive reaction was detected as brown to black intracellular granular accumulations. All sections were mounted in DPX mounting medium (Sigma-Aldrich) and examined using a DMLB microscope (Leica Microsystems, Wetzlar, Germany).

2.3.2 Immunohistochemistry and immunofluorescence

To determine the expression and localization of insulin, glucagon, pancreas/duodenum homeobox protein 1 (PDX-1), 4-hydroxynonenal (4-HNE), Nrf2 and its downstream targets: GPX4, xCT, heme oxygenase-1 (HO-1) and peroxiredoxin-2 (PRDX-2) in the endocrine pancreas, immunohistochemical or immunofluorescence staining was performed. To analyze the localization of α- and β-cells, a comparative analysis of serial tissue sections immunostained against insulin and glucagon (i.e., "mirror" technique) was performed. Five µm thick pancreatic sections were deparaffinized with xylene and rehydrated in graded ethanol. Antigen retrieval in citrate buffer (pH 6.6, microwave boiling, 5 min), blocking of endogenous peroxidase activity (3% H_2O_2 in methanol, 10 min), and blocking of nonspecific binding with bovine serum albumin (5% BSA in PBS, 30 min) were performed before incubation of primary antibodies. Samples were incubated overnight at 4°C with the following primary antibodies diluted in 1% BSA in PBS: rabbit anti-insulin (1:100, sc-9168, Santa Cruz Biotechnology, TX, USA), anti-glucagon (1:300, sc-13091, Santa Cruz Biotechnology), anti PDX-1 (1:1000; sc-25403, Santa Cruz Biotechnology), anti-4-HNE (ab46545, 1:500; Abcam, Cambridge, UK), anti-Nrf2 (ab31163, 1:100, Abcam), anti-GPX4 (ab125066, 1:100, Abcam), anti-HO-1 (ab13243, 1.25:1000, Abcam) and mouse anti-PRDX-2 (sc-515428, 1:200, Santa Cruz Biotechnology). After rinsing with PBS, the sections were incubated with secondary goat anti-rabbit or anti-mouse antibody, depending on the host of the primary antibody (ab97051 and ab6789, 1:1000, Abcam, UK) for one hour at room temperature. The final reaction product was visualized after incubation in DAB chromogen solution (K 3408, Dako liquid

DAB+ Substrate Chromogen Substrate System, Agilent Technologies, Santa Clara, CA, USA). After counterstaining with hematoxylin, slides were mounted in DPX and examined with a light microscope (Leica Microsystems). For the quantification of immunopositivity of islets to Nrf2, GPX4, 4-HNE, HO-1, PDX-1 and PRDX-2, Color deconvolution tool in Image J (NIH) was applied (H-DAB setup) and DAB (brown signal) images were used to determine mean grayscale value of islets per group. Arbitrary values were calculated as 1000/greyscale level to obtain a direct proportionality between the signal intensity and the values obtained. β- and α-cell ratio was calculated by counting insulin- and glucagon-positive cells in islets. The values were presented as number of cells per islet area (1000 µm²).

To detect the localization of xCT in pancreatic β-cells, double immunofluorescence labelling of xCT and insulin was performed. After routine deparaffinization, rehydration, antigen retrieval with citrate buffer, and protein blocking (5% normal goat serum in 1% BSA in PBS-Tween), the mixture of goat anti-xCT (1:40, sc79360, Santa Cruz Biotechnology) and rabbit anti-insulin antibodies (1:100, sc9168, Santa Cruz Biotechnology) was applied and incubated overnight at 4°C. After thorough washing, the sections were incubated with the appropriate secondary antibodies: anti-goat Alexa Fluor 488 (1:200; A-11055, Thermo Fisher Scientific, Waltham, MA, USA) and anti-rabbit Alexa Fluor 647 (1:200; ab 150079, Abcam). Antibodies were diluted in 1% BSA in PBS-Tween and incubated for 30 min at room temperature. After washing, sections were embedded in Mowiol (Sigma-Aldrich) and analysed on the SP5 confocal microscope (Leica Microsystems). Average xCT immunopositivity of β-cells was measured in LAS AF software (Leica Microsystems).

2.3.3 TUNEL staining

To determine whether cell death-related DNA fragmentation occurs *in situ* under diabetic conditions, fluorescent TUNEL staining (*In Situ* Cell Death Detection Kit, Fluorescein; Roche Applied-Science) was performed according to the manufacturer's protocol. After deparaffinization and rehydration, slides were incubated with proteinase K solution for 30 min at 37°C, washed in PBS for 2 min, and incubated with TUNEL reaction mixture for 1 h at 37°C after blocking. After washing, slides were counterstained with propidium iodide, washed, and mounted with Mowiol mounting medium (Sigma-Aldrich) for analysis on the SP5 confocal microscope (Leica Microsystems). Average nuclear TUNEL fluorescence intensity of islet cells was measured in LAS AF software (Leica Microsystems).

2.4 Statistical analysis

Statistical analysis was performed using GraphPad Prism software (GraphPad Software, San Diego, CA, USA). To test the data for normality, the Kolmogorov-Smirnov test was used. If the F test indicated an overall difference, one-way analysis of variance (one-way ANOVA) was performed, followed by Tukey's multiple comparison test. Statistical significance was set at $p < 0.05$.

3 Results

As expected, at the end of the experiment (day 22), the mean serum glucose and insulin levels were significantly altered in the diabetic animals (Figures 1A, B). Concurrent treatment with Fer-1 slightly lowered the blood glucose level toward the control value, and significantly increased insulin level above the value measured in the diabetic group. Consistent with the serum glucose and insulin levels, a decrease in the mean islet size was less pronounced in the Fer-1-treated diabetic animals than in the untreated diabetic animals (Figure 1C). Additionally, fibrosis observed around and inside islets of diabetic mice also tended to decline toward control level of collagen depositions when treatment with Fer-1 was applied (Figures 1D, G),

Comparative immunohistochemical detection of insulin- and glucagon-positive cells in serial sections of pancreatic tissue showed fewer insulin-positive β-cells in the islets of diabetic mice than in the islets of control animals (Figures 1E, H). In addition, the proportion of glucagon-positive α-cells increased (Figure 1I), followed by their migration from the periphery of the islet to its center. Fer-1 treatment of diabetic mice significantly increased the proportion of insulin-positive cells. Moreover, the α-cells are slightly less numerous and more likely to be located in the periphery of the islets in this group.

Immunohistochemical detection of PDX-1 in islets of Langerhans showed a sharp decrease in its expression in diabetic mice (Figures 1F, J). In diabetic animals treated concomitantly with Fer-1, PDX-1 immunoexpression of islets increased, showing strong immunopositivity of the majority of islet cells, similar to that in controls. In addition, mild immunopositivity of exocrine acinar cells was detectable only in this group.

To detect signs of DNA fragmentation that might indicate the presence of dying cells, TUNEL staining was performed (Figure 2A). Although no signs of pyknosis or apoptotic bodies were detected in the islets of all groups, strong staining of the islet nuclei is evident in the DM group, indicating increased DNA fragmentation. Treatment with Fer-1 reduced this DNA damage, as evidenced by a lower TUNEL signal in the islet nuclei (Figures 2B). In addition, immunohistochemically, more 4-HNE adducts were noted in the endocrine pancreas of diabetic animals, indicating the increased lipid peroxidation (Figure 2D) as confirmed by the appearance of more islet cells with lipofuscin granules (Figure 2E). In these animals
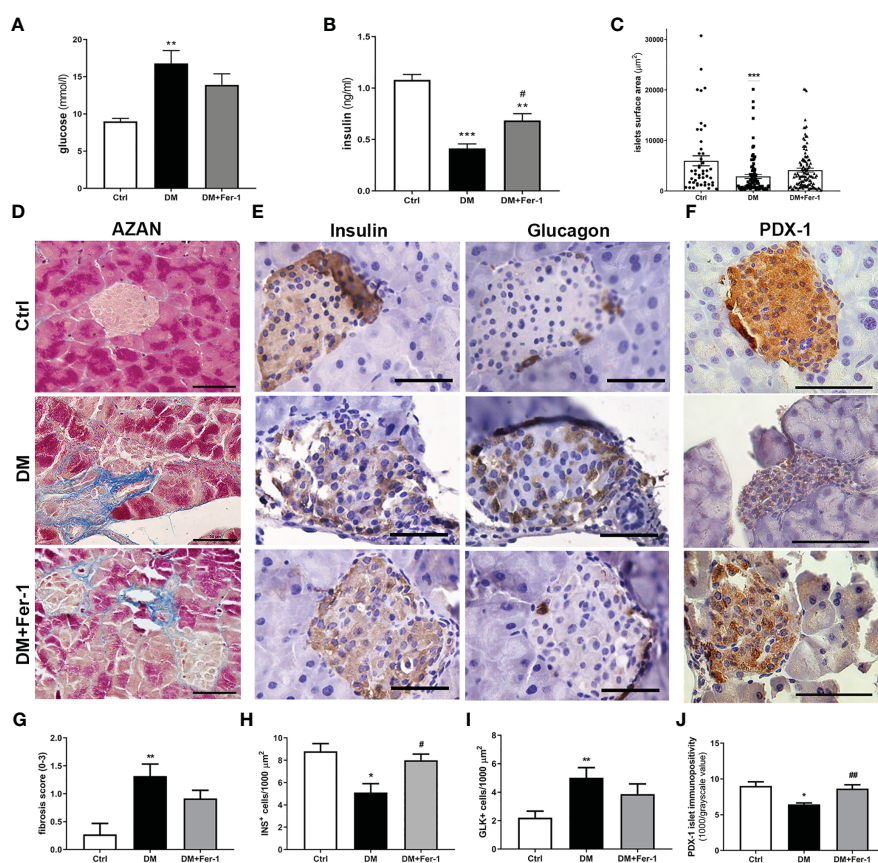

FIGURE 1
(A) Serum glucose levels and (B) serum insulin levels at day 22 of experiment; (C) islets surface area; (D) representative micrographs of islets, AZAN trichrome staining; (E) comparative immunohistochemical detection of insulin- and glucagon-positive cells at serial pancreatic sections; (F) immunohistochemical detection of PDX-1; (G) fibrosis score; (H) ratio of insulin-positive β (INS$^+$) and (I) glucagon-positive α cells (GLK$^+$); (J) average PDX-1 immunopositivity in islets of Langerhans from control (Ctrl), diabetic (DM), and Fer-1-treated diabetic animals (DM+Fer-1). Magnification and scale bar (D−F): ×40, 50 μm. Statistical significance (A−C, G−J): *p < 0.05, **p < 0.01, ***p < 0.001 − in comparison to Ctrl; #p < 0.05, ##p < 0.01 − in comparison to DM.
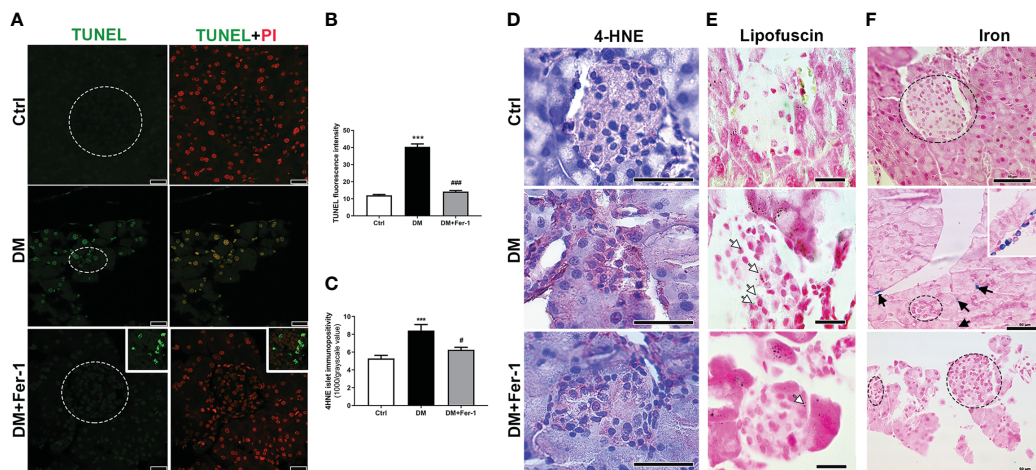
FIGURE 2
Detection of **(A)** DNA fragmentation (green, TUNEL staining) combined with PI staining of nuclei (red) in islets of Langerhans (encircled),
insert – a detail of a lymph node adjacent to pancreas; **(B)** quantification of DNA fragmentation inside islet nuclei (TUNEL fluorescence);
(C, D) immunohistochemical detection and quantification of 4-HNE in pancreatic islets from control (Ctrl), diabetic (DM), and Fer-1-treated diabetic
animals (DM +Fer-1); **(E)** Sudan III staining – lipofuscin detection inside islet cells (white arrows); **(F)** Pearl's staining – phagocytic iron (Fe^{3+})-loaded
cells in exocrine pancreas of diabetic animals (black arrows and insert) –iron-loaded cells;. Magnification and scale bar: **(A)** ×63, 25 μm; **(D, F)** ×40,
50 μm; **(E)** ×100, 20 μm.

pancreatic 4-HNE immunopositivity was particularly pronounced in the islets of Langerhans and blood vessels. Increased 4-HNE immunopositivity of islets was decreased by Fer-1 treatment, thusconfirming lower lipid peroxidation in the pancreas of these animals (Figure 2C). In addition, numerous phagocyte-like cells with iron-containing phagosomes/lysosomes were detectable in the pancreas of the diabetic animals (Figure 2F). Their presence was rarely detectable in Fer-1-treated diabetic animals. This indicates increased phagocytic activity in the pancreas of diabetic animals, which probably serves to ingest and remove dead islet cells.

Nrf2 and GPX4 immunopositivity of islet cells is shown in Figures 3A and B, respectively. A homogeneous distribution of Nrf2 immunopositivity is detectable in the islet cells of the control animals, with few Nrf2-positive nuclei. In the DM group, Nrf2 immunopositivity of islet cells decreased, whereas Fer-1 treatment of diabetic animals resulted in a sharp increase in Nrf2 immunopositivity that exceeded control level (Figure 3F), including more Nrf2-positive nuclei (Figure 3A **inset**). GPX4 immunopositivity of control islets is weak, although rim cells (which correspond to α-cells based on their localization) are somewhat more GPX4-positive. A similar pattern is seen in the diabetic group, with slightly increased immunopositivity of surrounding acinar cells (Figure 3B **inset**) in contrast to the DM +Fer-1 group, in which strong immunopositivity of all pancreatic endocrine tissue was detected. The differences in the islet immunopositivity to GPX4 among the groups was confirmed by the quantitative analysis (Figure 3G).

To analyze the xCT immunopositivity of the islet cells and to determine whether the experimental treatments used altered the expression of xCT in the β-cells, co-staining of xCT and insulin was performed (Figure 3C). As shown, islet cells from the control animals are strongly positive for xCT. In the islet cells of the diabetic animals, xCT immunopositivity decreased, with the

greatest decrease in β-cells, whereas Fer-1 treatment significantly increased immunoexpression in these cells, even above the control level (Figure 3H).

In addition to GPX4 and xCT, immunohistochemical detection of HO-1 and PRDX-2, the additional Nrf2 downstream targets, was performed (Figures 3D, E). The results showed a similar pattern for both antioxidant enzymes in the pancreatic islets, with decreased immunopositivity in the DM group, which reverted to control levels in most of the islets when DM animals were treated simultaneously with Fer-1 (Figures 3I, J)

4 Discussion

Previous evidence, including ours, suggests the involvement of ferroptosis in the development and progression of diabetes and diabetic complications (14–20). However, data on possible protective effects of antiferroptotic agents in β-cells *in vivo* are still unclear. To elucidate the mechanisms of islet of Langerhans deterioration in T1D and the benefits of using Fer-1 as an antiferroptotic agent in the treatment of this disease, a thorough microscopic examination of pancreatic tissue from diabetic mice was performed. The results of the present study are summarized graphically in Figure 4.

The analyses of serum levels of insulin and glucose showed the beneficial effects of Fer-1 in diabetic animals, as levels of both parameters changed toward control values. This is consistent with our previous results (14), in which it was shown that glycemia in diabetic animals treated with Fer-1 tended to recover to physiological levels. At the histological level, the reduced hyperglycemia is associated with a slight improvement in islet size and reduced infiltration of immune cells (insulitis/periinsulitis), as we also showed in our recent work (14). This is followed by a partial
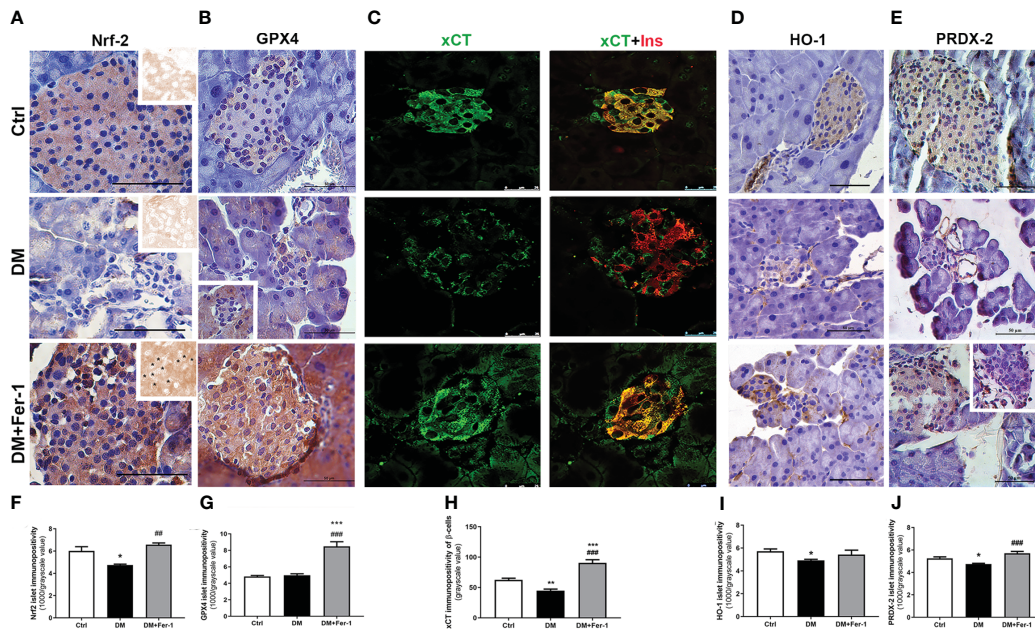
FIGURE 3

Immunohistochemical detection and quantification of islet immunopositivity to **(A, F)** Nrf2 (insets on **(A)** − DAB channel of the original images, asterisk showing Nrf2 nuclear immunopositivity) **(B, G)** GPX4, **(D, I)** HO-1 and **(E, J)** PRDX-2. Immunofluorescence colocalization of **(C)** xCT (green) and insulin (red) in islets of Langerhans from control (Ctrl), diabetic (DM), and Fer-1-treated diabetic animals (DM+Fer-1) and **(H)** xCT immunopositivity of β-cells. Magnification and scale bar: **(A, B, D, E)** ×40, 50 µm; **(C)** ×63, 25 µm. Statistical significance **(F−J)**: *$p < 0.05$, **$p < 0.01$, ***$p < 0.001$ − in comparison to Ctrl; ##$p < 0.01$, ###$p < 0.001$ − in comparison to DM.

restoration of the abundance of insulin-positive β-cells, followed by increased insulin immunopositivity of individual cells when compared to the control, presumably to compensate for the reduction in the number of β-cells.

Moreover, the diabetes-induced reduction of β-cells in islets of Langerhans is followed by the increased appearance of glucagon-positive α-cells migrating to the center of the islet. While this confirms the efficacy of the T1D model used, in which β-cells are

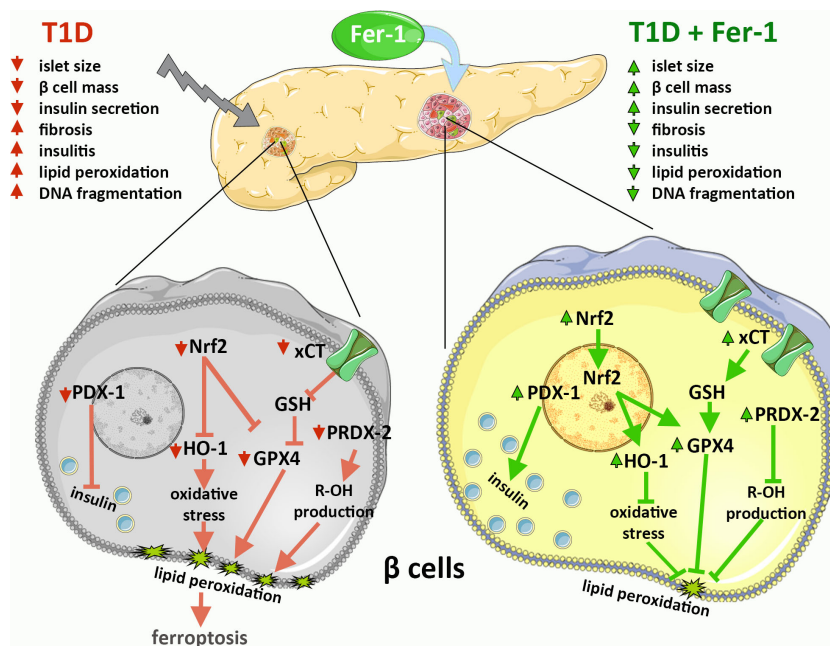
FIGURE 4

Graphical summary of the results on the contribution of β-cell ferroptosis to the development and pathogenesis of T1D via modulation of Nrf2 and its downstream targets and its inhibition by ferrostatin-1 (Fer-1).

selectively destroyed, it also argues for α-cell preservation or even hyperplasia, probably as a loss of insulin-driven paracrine action on neighboring α-cells (28, 29). The beneficial effects of Fer-1 treatment in T1D demonstrated in this study include normalization of the ratio and distribution of α- and β-cells in islets.

One of the parameters presented here for the first time, which speaks in favor of the beneficial effects of Fer-1 on β-cell survival and health is the restoration of PDX-1 protein immunoexpression to the control level. PDX-1 is considered as one of the major transcription factors involved in pancreatic development and maintenance of mature β-cell survival and function, including insulin synthesis and secretion (30–33). Its downregulation in β-cells in diabetes, has been shown to be involved in the dysfunction and death of β-cells (34–36).

After we have shown the improval of general parameters of β-cell mass and health in diabetic animals co-treated with Fer-1, we aimed to quest for the signs of cell death and proferroptotic damage in islets of diabetic animals as well as to investigate their eventual improval after the Fer-1 treatment. Despite a severe reduction in islet size and β-cell mass in the pancreas of diabetic mice, neither apoptotic nor necrotic cells were detected in islets of Langerhans by TUNEL staining. However, mild DNA fragmentation of islet cells was detected. This phenomenon is already described in diabetic β-cells and is implicated in the development and the exacerbation of both T1D and T2D (37, 38). The lack of morphologic evidence of dead islet cells could be explained by their rapid removal by phagocytes from the population of infiltrating immune cells (39, 40). Consistent with this suggestion, numerous macrophage-like cells loaded with iron depositions are found in the pancreas of diabetic mice. Fer-1 treatment however, improved both of these parameters, decreasing the signs of DNA damage of islet cells and presence of iron-loaded cells in the pancreatic tissue.

Further we have confirmed the increased accumulation of lipid peroxides in β-cells of diabetic animals, as demonstrated by increased lipofuscin accumulation and 4-HNE immunopositivity in pancreatic islet cells. The detected signs of islet cell damage, all of which were reduced by Fer-1, suggest the role of ferroptotic cell death in the elimination of β-cells in T1D, as previously shown in our study (14).

To confirm this assumption, an analysis of the immunoexpression and localization of the major contributors to the antiferroptotic pathway in the cell – Nrf2, GPX4, and xCT - was performed. From the literature, Nrf2 responds differently during the onset and progression of diabetes. Namely, in the early stages, Nrf2 is upregulated to respond to increased oxidative stress and overcome damage (41). In chronic hyperglycemia, sustained oxidative stress leads to inhibition of Nrf2 nuclear translocation, stimulation of Nrf2 degradation, and impaired activation of antioxidant genes, contributing to ROS accumulation (42–45). As shown here, on day 22 of the experiment immunoexpression of Nrf2 was reduced or even undetectable microscopically in islet cells of diabetic animals. Because Nrf2 is an antioxidant transcription factor involved in the metabolism of GSH (46–48), lipids (49) and iron (50, 51), its inactivation and/or suppression are considered important steps in the development and outcomes of ferroptosis (52). Consistent with decreased Nrf2 immunoexpression in islet

cells in diabetes, a similar pattern has been demonstrated for GPX4, a membrane-associated member of the GPX family (50) that is one of the major downstream target enzymes of Nrf2 activation. GPX4 immunoexpression was greatly reduced in centrally located islet cells (β-), whereas it was unchanged in marginal cells (α-). GPX4 is considered to be the major enzyme involved in the removal of ROS-driven membrane lipid peroxides in the context of ferroptotic cell death (5, 53, 54), as shown by others and our team (14, 15, 55–57). This enzyme has previously been shown to be highly expressed and important for the survival of β-cells (58), suggesting the importance of protecting these cells from oxidative degradation of their membrane lipids.

Along with the decrease of GPX4 protein expression in islets of diabetic animals, it seems evident that its lipid peroxide-removing capacity is impaired due to decreased GSH bioavailability as previously confirmed (59). Namely, there was also a decline in the protein expression of xCT in β-cells of diabetic mice, as evidenced by our immunofluorescence results. L-cystine import by xCT is considered the rate-limiting step in the GSH biosynthesis and GPX4 activity (5, 60).

To further investigate the effects of Nrf2 downregulation in islet cells, we additionally analysed the immunoexpression of HO-1 and PRDX-2 (61), Nrf2 downstream targets involved in antioxidant protection of β-cells and their survival. HO-1 plays an important role against iron-overload-induced stress (62–64), whereas PRDX-2 is a selenium-independent glutathione peroxidase that eliminates peroxides (65, 66). In the case of both enzymes, DM decreased their islet immunoexpression, which was restored by Fer-1.

Altogether, decrease in Nrf2, along with its downstream targets – GPX4, xCT and HO-1, followed by the accumulation of lipid peroxides (as discussed above) in islet cells, suggest ferroptosis as an important mode of β-cells removal in T1D. To our knowledge, the participation of PRDX-2 downregulation in ferroptosis of islet cells is demonstrated for the first time in diabetes, although PRDX family is already shown to protect different cells from ferroptosis (67).

Regarding the effects of Fer-1 on these main cellular contributors involved in the enzymatic degradation of membrane lipid peroxides in the islets of Langerhans of diabetic animals, we have demonstrated upregulated expression and increased nuclear translocation of Nrf2, thus demonstrating activation of the Nrf2 pathway by Fer-1. This was followed by the upregulated expression of GPX4, xCT, HO-1 and PRDX-2 in β-cells. To date, Fer-1 is known to be one of the most potent inhibitors of ferroptosis, exhibiting high potency as a free radical scavenging antioxidant, with particularly high potency in phospholipid bilayer membranes compared with other antioxidants (68), and the mechanism by which it activates Nrf2 is currently unknown but certainly worthy of further investigation. All of the mentioned improvements in Nrf2 signaling pathway argue for the observed antiferroptotic activity of Fer-1 in β-cells *in vivo*, which could be considered as a potential antidiabetic strategy to preserve their functionality and mass. The protective effects of Fer-1 in both diabetic endocrine pancreas and liver (14, 15), give us insight into its actions and allow the selection of additional feropttosis inhibitors in future studies, such as liproxtatin-1 which has been shown to be highly suitable for *in vivo* application (69). Overall, our *in vivo* microscopic study

confirms the important contribution of ferroptosis of β-cells in the development and pathogenesis of T1D via modulation of Nrf2 and its downstream targets. Moreover, our results suggest antiferroptotic agents as a promising therapeutic strategy for the prevention and treatment of diabetes.

Data availability statement

The raw data supporting the conclusions of this article will be made available by the authors, without undue reservation.

Ethics statement

The animal study was reviewed and approved by Ethics Committee of the Institute of Biological Research "Sinisa Stankovic", National Institute of Republic of Serbia, University of Belgrade, Belgrade, Serbia.

Author contributions

MM: methodology, validation, formal analysis, investigation, resources, writing - original draft preparation, review and editing, visualization. AS: conceptualization, methodology, validation, formal analysis, investigation, writing - review and editing, visualization. TS: methodology, resources, writing - review and editing. IG: conceptualization, formal analysis, resources, writing - review and editing. DM: methodology, investigation. KV: validation, resources, writing - review and editing. VM: validation, formal analysis. NS: methodology, investigation. AG:

investigation, formal analysis. VO: conceptualization, methodology, validation, investigation, resources, data curation, supervision, project administration, funding acquisition. All authors contributed to the article and approved the submitted version.

Funding

Conflict of interest

The authors declare that the research was conducted in the absence of any commercial or financial relationships that could be construed as a potential conflict of interest.

Publisher's note

All claims expressed in this article are solely those of the authors and do not necessarily represent those of their affiliated organizations, or those of the publisher, the editors and the reviewers. Any product that may be evaluated in this article, or claim that may be made by its manufacturer, is not guaranteed or endorsed by the publisher.

References

1. Galluzzi L, Bravo-San Pedro JM, Vitale I, Aaronson SA, Abrams JM, Adam D, et al. Essential versus accessory aspects of cell death: recommendations of the NCCD 2015. *Cell Death Differentiation.* (2015) 22(1):58–73. doi: 10.1038/cdd.2014.137

2. Galluzzi L, Bravo-San Pedro JM, Kepp O, Kroemer G. Regulated cell death and adaptive stress responses. *Cell Mol Life Sci* (2016) 73(11-12):2405–10. doi: 10.1007/s00018-016-2209-y

3. Galluzzi L, Vitale I, Aaronson SA, Abrams JM, Adam D, Agostinis P, et al. Molecular mechanisms of cell death: recommendations of the Nomenclature Committee on Cell Death 2018. *Cell Death Differ* (2018) 25(3):486–541. doi: 10.1038/s41418-017-0012-4

4. Dixon SJ, Lemberg KM, Lamprecht MR, Skouta R, Zaitsev EM, Gleason CE, et al. Ferroptosis: an iron-dependent form of nonapoptotic cell death. *Cell* (2012) 149 (5):1060–72. doi: 10.1016/j.cell.2012.03.042

5. Yang WS, SriRamaratnam R, Welsch ME, Shimada K, Skouta R, Viswanathan VS, et al. Regulation of ferroptotic cancer cell death by GPX4. *Cell* (2014) 156(1-2):317–31. doi: 10.1016/j.cell.2013.12.010

6. Dixon SJ, Patel DN, Welsch M, Skouta R, Lee ED, Hayano M, et al. Pharmacological inhibition of cystine-glutamate exchange induces endoplasmic reticulum stress and ferroptosis. *Elife* (2014) 3:e02523. doi: 10.7554/eLife.02523

7. Sato H, Tamba M, Ishii T, Bannai S. Cloning and expression of a plasma membrane cystine/glutamate exchange transporter composed of two distinct proteins. *J Biol Chem* (1999) 274(17):11455–8. doi: 10.1074/jbc.274.17.11455

8. Lewerenz J, Hewett SJ, Huang Y, Lambros M, Gout PW, Kalivas PW, et al. The cystine/glutamate antiporter system x(c)(-) in health and disease: from molecular mechanisms to novel therapeutic opportunities. *Antioxid Redox Signal* (2013) 18 (5):522–55. doi: 10.1089/ars.2011.4391

9. Ursini F, Maiorino M. Lipid peroxidation and ferroptosis: The role of GSH and GPx4. *Free Radical Biol Med* (2020) 152:175–85. doi: 10.1016/j.freeradbiomed.2020.02.027

10. Shah R, Shchepinov MS, Pratt DA. Resolving the role of lipoxygenases in the initiation and execution of ferroptosis. *ACS Cent Sci* (2018) 4(3):387–96. doi: 10.1021/acscentsci.7b00589

11. Wenzel SE, Tyurina YY, Zhao J, St Croix CM, Dar HH, Mao G, et al. PEBP1 wardens ferroptosis by enabling lipoxygenase generation of lipid death signals. *Cell* (2017) 171(3):628–41.e26. doi: 10.1016/j.cell.2017.09.044

12. Anandhan A, Dodson M, Shakya A, Chen J, Liu P, Wei Y, et al. NRF2 controls iron homeostasis and ferroptosis through HERC2 and VAMP8. *Sci Adv* (2023) 9(5): eade9585. doi: 10.1126/sciadv.ade9585

13. Stockwell BR, Jiang X, Gu W. Emerging mechanisms and disease relevance of ferroptosis. *Trends Cell Biol* (2020) 30(6):478–90. doi: 10.1016/j.tcb.2020.02.009

14. Stancic A, Saksida T, Markelic M, Vucetic M, Grigorov I, Martinovic V, et al. Ferroptosis as a novel determinant of beta-cell death in diabetic conditions. *Oxid Med Cell Longev* (2022) 2022:3873420. doi: 10.1155/2022/3873420

15. Stancic A, Velickovic K, Markelic M, Grigorov I, Saksida T, Savic N, et al. Involvement of ferroptosis in diabetes-induced liver pathology. *Int J Mol Sci* (2022) 23 (16). doi: 10.3390/ijms23169309

16. Feng X, Wang S, Sun Z, Dong H, Yu H, Huang M, et al. Ferroptosis Enhanced Diabetic Renal Tubular Injury via HIF-1α/HO-1 Pathway in db/db Mice. *Front Endocrinol* (2021) 12. doi: 10.3389/fendo.2021.626390

17. Kim S, Kang SW, Joo J, Han SH, Shin H, Nam BY, et al. Characterization of ferroptosis in kidney tubular cell death under diabetic conditions. *Cell Death Dis* (2021) 12(2):160. doi: 10.1038/s41419-021-03452-x

18. Hao L, Mi J, Song L, Guo Y, Li Y, Yin Y, et al. SLC40A1 mediates ferroptosis and cognitive dysfunction in type 1 diabetes. *Neuroscience* (2021) 463:216–26. doi: 10.1016/j.neuroscience.2021.03.009

19. Ma H, Wang X, Zhang W, Li H, Zhao W, Sun J, et al. Melatonin suppresses ferroptosis induced by high glucose via activation of the Nrf2/HO-1 signaling pathway in type 2 diabetic osteoporosis. *Oxid Med Cell Longevity.* (2020) 2020:9067610. doi: 10.1155/2020/9067610

20. Luo EF, Li HX, Qin YH, Qiao Y, Yan GL, Yao YY, et al. Role of ferroptosis in the process of diabetes-induced endothelial dysfunction. *World J Diabetes.* (2021) 12 (2):124–37. doi: 10.4239/wjd.v12.i2.124

21. Mukherjee N, Lin L, Contreras CJ, Templin AT. β-cell death in diabetes: past discoveries, present understanding, and potential future advances. *Metabolites* (2021) 11(11). doi: 10.3390/metabo11110796

22. Kim KA, Lee MS. Role and mechanism of pancreatic β-cell death in diabetes: The emerging role of autophagy. *J Diabetes Investig* (2010) 1(6):232–8. doi: 10.1111/j.2040-1124.2010.00054.x

23. Miotto G, Rossetto M, Di Paolo ML, Orian L, Venerando R, Roveri A, et al. Insight into the mechanism of ferroptosis inhibition by ferrostatin-1. *Redox Biol* (2020) 28:101328. doi: 10.1016/j.redox.2019.101328

24. Lenzen S, Drinkgern J, Tiedge M. Low antioxidant enzyme gene expression in pancreatic islets compared with various other mouse tissues. *Free Radic Biol Med* (1996) 20(3):463–6. doi: 10.1016/0891-5849(96)02051-5

25. Tonooka N, Oseid E, Zhou H, Harmon JS, Robertson RP. Glutathione peroxidase protein expression and activity in human islets isolated for transplantation. *Clin Transplant.* (2007) 21(6):767–72. doi: 10.1111/j.1399-0012.2007.00736.x

26. Jovanovic Stojanov S, Martinovic V, Bogojevic D, Poznanovic G, Petrovic A, Ivanovic-Matic S, et al. Modulation of diabetes-related liver injury by the HMGB1/TLR4 inflammatory pathway. *J Physiol Biochem* (2018) 74(2):345–58. doi: 10.1007/s13105-018-0626-0

27. Kim J-W, Park S-Y, You Y-H, Ham D-S, Lee S-H, Yang HK, et al. Suppression of ROS production by exendin-4 in PSC attenuates the high glucose-induced islet fibrosis. *PloS One* (2016) 11(12):e0163187. doi: 10.1371/journal.pone.0163187

28. Rodriguez-Diaz R, Molano RD, Weitz JR, Abdulreda MH, Berman DM, Leibiger B, et al. Paracrine interactions within the pancreatic islet determine the glycemic set point. *Cell Metab* (2018) 27(3):549–58.e4. doi: 10.1016/j.cmet.2018.01.015

29. Hartig SM, Cox AR. Paracrine signaling in islet function and survival. *J Mol Med (Berl)* (2020) 98(4):451–67. doi: 10.1007/s00109-020-01887-x

30. Fujimoto K, Polonsky KS. Pdx1 and other factors that regulate pancreatic beta-cell survival. *Diabetes Obes Metab* (2009) 11 Suppl 4(Suppl 4):30–7. doi: 10.1111/j.1463-1326.2009.01121.x

31. Offield MF, Jetton TL, Labosky PA, Ray M, Stein RW, Magnuson MA, et al. PDX-1 is required for pancreatic outgrowth and differentiation of the rostral duodenum. *Development* (1996) 122(3):983–95. doi: 10.1242/dev.122.3.983

32. Gao T, McKenna B, Li C, Reichert M, Nguyen J, Singh T, et al. Pdx1 maintains β cell identity and function by repressing an α cell program. *Cell Metab* (2014) 19 (2):259–71. doi: 10.1016/j.cmet.2013.12.002

33. Jonsson J, Carlsson L, Edlund T, Edlund H. Insulin-promoter-factor 1 is required for pancreas development in mice. *Nature* (1994) 371(6498):606–9. doi: 10.1038/371606a0

34. Kaneto H, Matsuoka TA. Down-regulation of pancreatic transcription factors and incretin receptors in type 2 diabetes. *World J Diabetes.* (2013) 4(6):263–9. doi: 10.4239/wjd.v4.i6.263

35. Sachdeva MM, Claiborn KC, Khoo C, Yang J, Groff DN, Mirmira RG, et al. Pdx1 (MODY4) regulates pancreatic beta cell susceptibility to ER stress. *Proc Natl Acad Sci* (2009) 106(45):19090–5. doi: 10.1073/pnas.0904849106

36. Li SW, Koya V, Li Y, Donelan W, Lin P, Reeves WH, et al. Pancreatic duodenal homeobox 1 protein is a novel beta-cell-specific autoantigen for type I diabetes. *Lab Invest.* (2010) 90(1):31–9. doi: 10.1038/labinvest.2009.116

37. Horwitz E, Krogvold L, Zhitomirsky S, Swisa A, Fischman M, Lax T, et al. β-cell DNA damage response promotes islet inflammation in type 1 diabetes. *Diabetes* (2018) 67(11):2305–18. doi: 10.2337/db17-1006

38. Shimizu I, Yoshida Y, Suda M, Minamino T. DNA damage response and metabolic disease. *Cell Metab* (2014) 20(6):967–77. doi: 10.1016/j.cmet.2014.10.008

39. Cosentino C, Regazzi R. Crosstalk between macrophages and pancreatic β-cells in islet development, homeostasis and disease. *Int J Mol Sci* (2021) 22(4):1765. doi: 10.3390/ijms22041765

40. Parv K, Westerlund N, Merchant K, Komijani M, Lindsay RS, Christoffersson G. Phagocytosis and efferocytosis by resident macrophages in the mouse pancreas. *Front Endocrinol (Lausanne).* (2021) 12:606175. doi: 10.3389/fendo.2021.606175

41. Abebe T, Mahadevan J, Bogachus L, Hahn S, Black M, Oseid E, et al. Nrf2/antioxidant pathway mediates β cell self-repair after damage by high-fat diet-induced oxidative stress. *JCI Insight* (2017) 2(24). doi: 10.1172/jci.insight.92854

42. Behl T, Kaur I, Sehgal A, Sharma E, Kumar A, Grover M, et al. Unfolding Nrf2 in diabetes mellitus. *Mol Biol Rep* (2021) 48(1):927–39. doi: 10.1007/s11033-020-06081-3

43. Soares MA, Cohen OD, Low YC, Sartor RA, Ellison T, Anil U, et al. Restoration of Nrf2 signaling norMalizes the regenerative niche. *Diabetes* (2016) 65(3):633–46. doi: 10.2337/db15-0453

44. Schultheis J, Beckmann D, Mulac D, Müller L, Esselen M, Düfer M. Nrf2 activation protects mouse beta cells from glucolipotoxicity by restoring mitochondrial function and physiological redox balance. *Oxid Med Cell Longev* (2019) 2019:7518510. doi: 10.1155/2019/7518510

45. Miller WP, Sunilkumar S, Giordano JF, Toro AL, Barber AJ, Dennis MD. The stress response protein REDD1 promotes diabetes-induced oxidative stress in the retina by Keap1-independent Nrf2 degradation. *J Biol Chem* (2020) 295(21):7350–61. doi: 10.1074/jbc.RA120.013093

46. Sasaki H, Sato H, Kuriyama-Matsumura K, Sato K, Maebara K, Wang H, et al. Electrophile response element-mediated induction of the cystine/glutamate exchange transporter gene expression *. *J Biol Chem* (2002) 277(47):44765–71. doi: 10.1074/jbc.M208704200

47. Lee JM, Calkins MJ, Chan K, Kan YW, Johnson JA. Identification of the NF-E2-related factor-2-dependent genes conferring protection against oxidative stress in primary cortical astrocytes using oligonucleotide microarray analysis. *J Biol Chem* (2003) 278(14):12029–38. doi: 10.1074/jbc.M211558200

48. Wu KC, Cui JY, Klaassen CD. Beneficial role of Nrf2 in regulating NADPH generation and consumption. *Toxicological Sci* (2011) 123(2):590–600. doi: 10.1093/toxsci/kfr183

49. Huang J, Tabbi-Anneni I, Gunda V, Wang L. Transcription factor Nrf2 regulates SHP and lipogenic gene expression in hepatic lipid metabolism. *Am J Physiology-Gastrointestinal Liver Physiol* (2010) 299(6):G1211–G21. doi: 10.1152/ajpgi.00322.2010

50. Kerins MJ, Ooi A. The roles of NRF2 in modulating cellular iron homeostasis. *Antioxid Redox Signal* (2018) 29(17):1756–73. doi: 10.1089/ars.2017.7176

51. Doll S, Conrad M. Iron and ferroptosis: A still ill-defined liaison. *IUBMB Life* (2017) 69(6):423–34. doi: 10.1002/iub.1616

52. Xie Y, Hou W, Song X, Yu Y, Huang J, Sun X, et al. Ferroptosis: process and function. *Cell Death Differentiation.* (2016) 23(3):369–79. doi: 10.1038/cdd.2015.158

53. Seibt TM, Proneth B, Conrad M. Role of GPX4 in ferroptosis and its pharmacological implication. *Free Radic Biol Med* (2019) 133:144–52. doi: 10.1016/j.freeradbiomed.2018.09.014

54. Ran Q, Liang H, Gu M, Qi W, Walter CA, Roberts LJ2nd, et al. Transgenic mice overexpressing glutathione peroxidase 4 are protected against oxidative stress-induced apoptosis. *J Biol Chem* (2004) 279(53):55137–46. doi: 10.1074/jbc.M410387200

55. Friedmann Angeli JP, Schneider M, Proneth B, Tyurina YY, Tyurin VA, Hammond VJ, et al. Inactivation of the ferroptosis regulator Gpx4 triggers acute renal failure in mice. *Nat Cell Biol* (2014) 16(12):1180–91. doi: 10.1038/ncb3064

56. Hambright WS, Fonseca RS, Chen L, Na R, Ran Q. Ablation of ferroptosis regulator glutathione peroxidase 4 in forebrain neurons promotes cognitive impairment and neurodegeneration. *Redox Biol* (2017) 12:8–17. doi: 10.1016/j.redox.2017.01.021

57. Sui X, Zhang R, Liu S, Duan T, Zhai L, Zhang M, et al. RSL3 drives ferroptosis through GPX4 inactivation and ROS production in colorectal cancer. *Front Pharmacol* (2018) 9. doi: 10.3389/fphar.2018.01371

58. Krümmel B, Plötz T, Jörns A, Lenzen S, Mehmeti I. The central role of glutathione peroxidase 4 in the regulation of ferroptosis and its implications for pro-inflammatory cytokine-mediated beta-cell death. *Biochim Biophys Acta Mol Basis Dis* (2021) 1867(6):166114. doi: 10.1016/j.bbadis.2021.166114

59. Dixon SJ. Ferroptosis: bug or feature? *Immunol Rev* (2017) 277(1):150–7. doi: 10.1111/imr.12533

60. Lewerenz J, Maher P. Control of redox state and redox signaling by neural antioxidant systems. *Antioxid Redox Signal* (2011) 14(8):1449–65. doi: 10.1089/ars.2010.3600

61. Baird L, Dinkova-Kostova AT. The cytoprotective role of the Keap1-Nrf2 pathway. *Arch Toxicol* (2011) 85(4):241–72. doi: 10.1007/s00204-011-0674-5

62. Tobiasch E, Günther L, Bach FH. Heme oxygenase-1 protects pancreatic beta cells from apoptosis caused by various stimuli. *J Investig Med* (2001) 49(6):566–71. doi: 10.2310/6650.2001.33721

63. Pileggi A, Molano RD, Berney T, Cattan P, Vizzardelli C, Oliver R, et al. Heme oxygenase-1 induction in islet cells results in protection from apoptosis and improved in *vivo* function after transplantation. *Diabetes* (2001) 50(9):1983–91. doi: 10.2337/diabetes.50.9.1983

64. Hamad M, Mohammed AK, Hachim MY, Mukhopadhy D, Khalique A, Laham A, et al. Heme Oxygenase-1 (HMOX-1) and inhibitor of differentiation proteins (ID1, ID3) are key response mechanisms against iron-overload in pancreatic β-cells. *Mol Cell Endocrinol* (2021) 538:111462. doi: 10.1016/j.mce.2021.111462

65. Zhao F, Wang Q. The protective effect of peroxiredoxin II on oxidative stress induced apoptosis in pancreatic β-cells. *Cell Bioscience* (2012) 2(1):22. doi: 10.1186/2045-3701-2-22

66. Stancill JS, Corbett JA. The role of thioredoxin/peroxiredoxin in the β-cell defense against oxidative damage. *Front Endocrinol (Lausanne).* (2021) 12:718235. doi: 10.3389/fendo.2021.718235

67. Tang D, Chen X, Kang R, Kroemer G. Ferroptosis: molecular mechanisms and health implications. *Cell Res* (2021) 31(2):107–25. doi: 10.1038/s41422-020-00441-1

68. Zilka O, Shah R, Li B, Friedmann Angeli JP, Griesser M, Conrad M, et al. On the mechanism of cytoprotection by ferrostatin-1 and liproxstatin-1 and the role of lipid peroxidation in ferroptotic cell death. *ACS Cent Sci* (2017) 3(3):232–43. doi: 10.1021/acscentsci.7b00028

69. Stockwell BR, Jiang X. The chemistry and biology of ferroptosis. *Cell Chem Biol* (2020) 27(4):365–75. doi: 10.1016/j.chembiol.2020.03.013